Lubricant-Oil-Dispersible Stainless-Steel-Binding Block Copolymer Nanoaggregates and Nanospheres

Ronghua Zheng, Jiandong Wang, and Guojun Liu*

Department of Chemistry, Queen's University, 90 Bader Lane, Kingston, Ontario, Canada K7L 3N6

Tze-Chi Jao

Fundamental Research Group, Afton Chemical Corporation, 500 Spring Street, Richmond, Virginia 23219

Received April 17, 2007; Revised Manuscript Received July 5, 2007

ABSTRACT: Nanoaggregates were prepared from five samples of poly[(2-ethylhexyl acrylate)-*ran*-(*tert*-butyl acrylate)]-*block*-poly(2-cinnamoyloxyethyl acrylate), P(EXA−tBA)−PCEA in block-selective solvents for P(EXA−tBA). The effect of varying diblock composition, block-selective solvent, and equilibrium temperature on the size and shape of the nanoaggregates formed was investigated. Nanospheres were obtained after the photo-cross-linking of the spherical nanoaggregates. The tBA groups in the corona of these nanospheres could be hydrolyzed to give P(EXA−tBA−AA), where AA denotes acrylic acid, with a controlled fraction of AA units. Nanospheres with low contents of AA groups in their corona disperse well in low-polarity solvents and bind effectively to stainless-steel surfaces.

I. Introduction

In a block-selective solvent a diblock copolymer forms micelles or nanoaggregates with the soluble block making up the corona and the insoluble block making up the core, where the term "nanoaggregate" is more loose and bears no connotation on the stability origin of the aggregate formed and the term "micelle" denotes a nanoaggregate that is thermodynamically stable under a given set of conditions. Nanoaggregate and micelle formation from block copolymers in block-selective solvents has been studied extensively over the past four decades.[1−5] Efforts of the past decade have been directed mainly to the study of multiple morphology,[6−14] morphological transition,[15−17] and size control[18−21] of block copolymer nanoaggregates. By changing parameters such as the relative length of the soluble and insoluble blocks of a diblock and the block-selective solvent, one can effect formation of block copolymer nanoagregates with tens of morphologies ranging from spheres[1] to cylinders,[6,8,22] vesicles,[6,23] donuts,[8,11,13] etc. The two parameters can be changed also to tune the size of the nanoaggregates. Despite many prior studies, we failed to find in the literature formulations for block copolymer nanoaggregates that not only disperse in lubricant oils but also bind effectively to stainless-steel surfaces because these two requirements are conflicting. While dispersion in lubricant oils requires nonpolar polymers[24] for the low polarity of the oils, which typically consist of paraffins, aromatics, and naphthalenes,[25] steel binding typically requires relatively polar segments. Reported in this paper are the preparation and characterization of nanoaggregates and cross-linked nanoaggregates that disperse well in lubricant oils and bind effectively to stainless-steel surfaces. Also reported are factors affecting the size and shape of the nanoaggregates formed.

We prepared such "hooky" or "sticky" nanoparticles because they might function well as a friction-reduction additive in lubricant oils. Traditionally, surfactants such as glyceryl monolaurate have been used as friction reduction agent because such amphiphiles avoid the direct contact of asperities of the opposing moving surfaces of two machine parts, which are made typically from stainless steel, by forming a film on the metal surfaces.[25−27] If not protected and in the so-called boundary lubrication regime where the opposing surfaces move slowly relative to one another and the mechanic load is high, protrusions of one surface are pushed into the other, and relative motion is possible only if these protrusions can plow through the opposing surface or are dulled. Such direct metal/metal contact is substantially reduced for surfactant-coated surfaces, and much less force or friction is experienced to slide the surfaces because shredding off such an adsorbed film is much easier than the metal pieces. While surfactants work well, a densely adsorbed diblock copolymer nanoaggregate or cross-linked nanoaggregate layer or even a star polymer layer might work better because such a layer could be much thicker depending on the size of the aggregates, as illustrated in Scheme 1.

As reported in the previous paper in this series,[28] we have identified and synthesized a family of poly[(2-ethylhexyl acrylate)-*ran*-(*tert*-butyl acrylate)]-*block*-poly(2-cinnamoyloxyethyl acrylate) or P(EXA−tBA)−PCEA polymers for this project (see Chart 1). P(EXA−tBA) with mostly EXA was chosen as the first block of the diblock because copolymers of EXA are being used in engine oils as a viscosity index improver, and PEXA is oil-soluble and thermally stable.[29] PCEA was used for its low solubility in lubricant oils and should thus facilitate micelle or nanoaggregate formation from the diblocks in such oils. PCEA, being photo-cross-linkable,[30] should also allow the structural locking of the nanoaggregates formed and enable lubrication performance studies of the particles at various temperatures without worrying about possible disintegration of the aggregates. A small amount, e.g., <2 mol %, of tBA was incorporated into the oil-soluble block because the tBA groups were to be hydrolyzed into acrylic acid (AA) groups[31,32] to facilitate adsorption of the nanoaggregates on to surfaces of stainless steel without compromising the dispersion of the particles in lubricant oils.

* Corresponding author. E-mail: guojun.liu@chem.queensu.ca.

10.1021/ma070901t CCC: $37.00
Published on Web 09/25/2007

Scheme 1. Schematic Illustration of How Adsorption of Sticky Nanospheres on Metal Surfaces Prevents the Direct Contact of Asperities of Two Rough Metal Surfaces

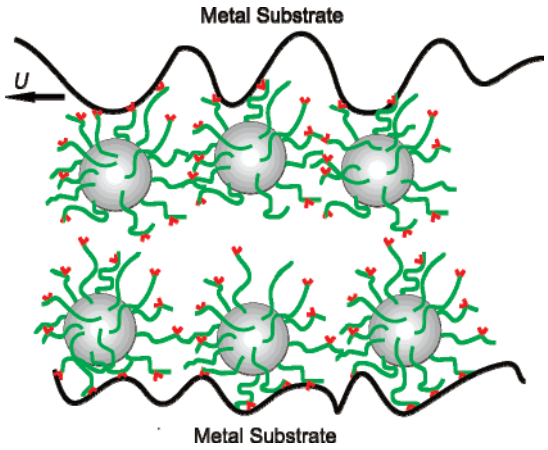

II. Experimental Section

Materials. Cyclohexane (CH, ≥99%), dodecane (≥99%), dioctyl ether (99%, bp = 286−287 °C), and hexane (99.9%) were purchased from Aldrich and were used as received. Stabilizer-free tetrahydrofuran from Fisher was purified by filtration through two alumina columns of an Innovation Technologies solvent purification system. Lubricant base oil EHC-45 was a product of Imperial Oil and supplied by Afton Chemical Corp. It is a hydrocracked group II base oil with high saturated hydrocarbon content (95%) and low volatility. Our experiments yielded a refractive index of 1.4667 at the sodium D line and a viscosity[33] of 36.3 cP at 22 °C for the oil. The five P(EXA−tBA)−PCEA samples used in this study are denoted as P1, P2, P3, P4, and P5, respectively, and their molecular characteristics are presented in the Results and Discussion section.

Nanoaggregate Preparation. Two methods were used to prepare the nanoaggregates. Method 1 involved dispersing directly P(EXA−tBA)−PCEA in hot singular block-selective solvents such as CH. An example procedure involved adding 203 mL of CH into a flask containing 3.66 g of P4. The mixture was stirred at 60 °C overnight to obtain spherical nanoaggregates.

Method 2 involved dissolving a diblock in a solvent such as THF which is good for both P(EXA−tBA) and PCEA and then adding block-selective solvent slowly. In an example preparation, we started by dissolving 2.65 g of P1 in 26.5 mL of THF. Then added dropwise from a dropping funnel was 105.9 mL of CH under magnetic stirring to effect nanoaggregate formation.

Nanoaggregate Cross-Linking. Nanospheres were prepared after structurally locking in spherical P(EXA−tBA)−PCEA aggregates by photo-cross-linking the PCEA core. To obtain nanospheres from P1 nanoaggregates prepared in THF/CH mentioned above, the sample after equilibrium under stirring overnight at room temperature was transferred into a photolysis cell that was thermostated at 20 °C. The sample was irradiated under constant magnetic stirring with a UV beam, from a 500 W mercury lamp, that had passed a 270 nm cutoff filter for 46 h to afford a CEA double-bond conversion of 37% as determined from CEA double-bond absorbance decrease at 274 nm.[30]

Hydrolysis of tBA. Full hydrolysis of tBA of the P(EXA−tBA)−PCEA nanospheres was achieved by stirring the samples in methylene chloride and trifluoroacetic acid (TFA) at v/v = 75/25 for 3 h in the presence of 2.5 molar equiv of triethylsilane relative to tBA.[34] Partial hydrolysis of tBA was achieved in CH_2Cl_2/TFA at v/v = 95/5 using triethylsilane as the cation scavenger by varying the hydrolysis time. To establish the hydrolysis kinetics, we used a P5 P(EXA−tBA)−PCEA nanosphere sample that contained 6 mol % of tBA in the P(EXA−tBA) block. The preparation of one kinetic sample involved first dispersing 30 mg of the nanospheres in a vial containing 6.0 mL of CH_2Cl_2. To it were then added 0.51 μL of triethylsilane and 0.33 mL of trifluoroacetic acid. The mixture was stirred for a predesignated time before 1.5 mL of methanol was added to terminate the hydrolysis reaction. The mixture was then immediately concentrated and added into methanol to precipitate the nanospheres. The nanospheres were washed by methanol thrice and dried in a vacuum oven at room temperature for 20 h before NMR analysis in $CDCl_3$ of the degree of tBA hydrolysis. Other samples with different tBA hydrolysis times were prepared similarly.

Fluid Atomic Force Microscopy Measurements. Stainless-steel plates, grade 308 with mirrorlike #8 finishing on one side, were purchased from McMaster-Carr, Chicago, and were cut into 6 × 6 mm^2 pieces. Before use, the protective covering on the polished side was removed, and the pieces were carefully placed at the bottom of a beaker. To the beaker was then added a 2% aqueous Micro-90 cleaning solution (International Products).[35] The beaker content was heated at 60 °C for 20 min before the solution was decanted, and the polished surfaces of the stainless-steel pieces were lightly rubbed by cosmetic cotton balls to remove glue. This was followed by rinsing the pieces by deionized water, and the surfaces were dried by nitrogen passed through a 0.1 μm filter (Whatman Inc.).

P(EXA−tBA)−PCEA or P(EXA−tBA−AA)−PCEA P3 nanospheres were dispersed in dioctyl ether at 0.5−5.0 mg/mL after stirring overnight and ultrasonication for 20 s. For AFM specimen preparation, 6−8 drops of such a solution were dispensed on a cleaned stainless-steel square. The square was covered by a Petri dish (without covering we determined a 5 wt % dioctyl ether loss after 4 h due to evaporation) and left to stand for a given amount of time before imaging in the submerged state by a Veeco Bioscope mounted on an inverted Nikon fluorescence microscope supported on an air table. The controller used was Veeco IIIa, and the Veeco DNP silicon nitride tips used possessed a force constant of ∼0.6 N/m. Tapping-mode AFM was done at a resonance frequency ∼9 kHz.

Other Analytical Techniques. UV absorbances were measured on a Perkin-Elmer Lambda 2 instrument, and transmission electron microscopy (TEM) was performed on a Hitachi-7000 instrument. TEM samples were obtained by aspirating a fine mist of a dilute solution of an aggregate or nanosphere sample onto a carbon-coated copper grid using a home-built device.[16] The samples were stained by OsO_4 vapor for 1 h before observation. PCEA core sizes of the spherical or cylindrical aggregates were obtained from the average of at least 50 readings that were obtained manually.

Ambient atomic force microscopy (AFM) measurements were performed on a Veeco multimode microscope equipped with a IIIa controller. The tips used had force constant and oscillation frequency ca. 40 N/m and ca. 300 kHz, respectively. The tip radius was <5 nm. The specimens were prepared by aspirating a nanoaggregate or nanosphere solution on to a freshly cleaved mica substrate.

Dynamic Light Scattering. Dynamic light scattering (DLS) data were obtained from a Brookhaven model 9025 instrument using a He−Ne laser operated at 632.8 nm. The scattering angle used was 90°. All measurements were done at 22 °C, and the samples at ∼0.5 mg/mL were clarified by filtration through 0.45 μm filters (Whatman, Inc.). The data were treated by the cumulant method[36] to yield the average hydrodynamic diameter d_h and polydispersity K_2^2/K_4 for the nanoaggregates or nanospheres.

For d_h calculations refractive indices at the sodium D line and viscosity of solvents at 25 °C were used. The viscosity and refractive indices of THF/CH mixtures were the volume-weighted averages of those of the individual components. To compare d_h values of P3 nanoaggregates formed in different singular solvents, the aggregates were photo-cross-linked to a CEA double-bond conversion of ∼36% before dialysis against THF to achieve solvent switch. The final measurements were done in THF/CH with a CH volume fraction f_{CH} of 95%.

P3 Nanospheres with Different AA Contents. Nanoaggregates of P3 were prepared by dispersing 0.41 g of P3 in 41 mL of CH at 60 °C overnight. The sample was then irradiated with UV light to yield nanospheres with a CEA double-bond conversion of 43%. The solution was concentrated to 4 mL and added into 100 mL of

Chart 1

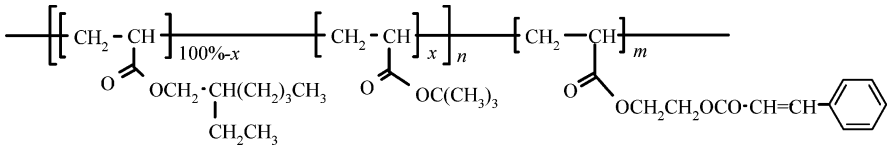

Table 1. Characteristics of the P(EXA-*r*-tBA)−PCEA Samples Used

sample	LS $10^{-4}M_w$ (g/mol)	SEC M_w/M_n	NMR n/m	n_w	m_w	x (%)	w_{PCEA} (%)
P1	8.6	1.24	1.53	235	150	1.5	47
P2	9.8	1.24	1.73	275	160	1.5	44
P3	15.8	1.27	0.82	335	410	0.5	62
P4	10.4	1.16	2.38	320	135	0.1	36
P5		1.34	0.62	∼150	∼235	6.0	69

methanol to precipitate the nanospheres. The nanospheres were dried under vacuum.

The P3 nanospheres were divided into five portions with one part not going through tBA hydrolysis. Samples with 20%, 40%, and 60% of tBA groups hydrolyzed were obtained by stirring the nanospheres in CH_2Cl_2/TFA at v/v = 95/5 containing triethylsilane for 29, 139, and 335 min, respectively. P3 nanospheres with tBA groups fully hydrolyzed were obtained from stirring the nanospheres in CH_2Cl_2/TFA at v/v = 75/25 containing triethylsilane for 3 h. The hydrolyzed spheres were purified by precipitation into methanol and were dried under vacuum.

The dried nanospheres, ∼5.6 mg for each sample, were stirred in 0.22 mL of THF overnight and then ultrasonicated for 1 min before 11.2 mL of dodecane was added under vigorous stirring. The THF was removed under rota-evaproation at 2.5 mmHg for 0.5 h. The dodecane solutions were stirred for 48 h before DLS measurements.

III. Results and Discussion

P(EXA−tBA)−PCEA Diblocks. Formation and properties of nanoaggregates from five P(EXA−tBA)−PCEA diblocks are discussed in this paper. The synthesis and characterization of these diblocks have been reported before.[28] The precursor P(EXA−tBA)−P(HEA−TMS), where P(HEA−TMS) denotes poly(2-trimethylsiloxyethyl acrylate), was prepared by sequential atom transfer radical polymerization.[37] The P(HEA−TMS) block was then hydrolyzed, and the resultant poly(2-hydroxyethyl acrylate) or PHEA block was reacted with cinnamoyl chloride to yield PCEA.[38]

The polymers except P5 were all characterized by light scattering (LS) to obtain the weight-average molar masses M_w and size exclusion chromatography (SEC) to yield the polydispersity index M_w/M_n in terms of polystyrene standards. The number of repeat unit ratios between the P(EXA−tBA) and PCEA blocks n/m were established from ^{1}H NMR analyses of the diblocks. Combining the LS M_w and NMR n/m values allowed calculation of the weight-average numbers of repeat units n_w and m_w. The tBA molar fraction x in the P(EXA−tBA) block was determined by ^{1}H NMR for P5 and was assumed to be the same as the tBA molar feed ratio for P1 to P4 because these values were too low to be determined accurately by NMR. Results of such characterizations are shown in Table 1. All of the samples used except P5 are low in polydispersity. The n/m values ranged from 0.82 to 2.38 with PCEA weight fraction w_{PCEA} changing from 36% to 62% for samples P1 to P4.

P5 was not characterized to the same rigor as the other samples because its aggregates were not used in lubrication tests. For lack of a LS M_w value, the n_w and m_w values for this sample were estimated on the basis of the monomer-to-initiator feed ratio, monomer conversion, and SEC M_w/M_n. Characteristics of this sample were included in Table 1 because it was used to establish tBA hydrolysis kinetics.

Nanoaggregate Preparation. PEXA is less polar than PCEA as judged by the solubility parameters δ of 17.8 and 20.2 MPa$^{1/2}$ for them calculated on the basis of group contributions to the molar cohesive energy and volume of the polymers.[39] Experimentally, we established that a P(EXA-*r*-tBA) sample with ∼200 repeat units and 1.5% tBA dissolved in many low-polarity solvents including hexane, cyclohexane, dodecane, and dioctyl ether with calculated δ parameters equal to 16.1, 17.6, 16.8, and 16.8 MPa$^{1/2}$, respectively, as well as in EHC-45 oil. In contrast, a PCEA sample with 120 units did not dissolve in any of the above solvents.

Nanoaggregates were prepared from P(EXA−tBA)−PCEA in P(EXA−tBA)-selective solvents in two ways. In approach 1, the diblocks were heated in a solvent directly to effect their dispersion. In approach 2, the diblocks were dissolved in a solvent such as THF or methylene chloride that is good for both P(EXA−tBA) and PCEA, and to such a solution was then added a block-selective solvent. To prepare nanoaggregates from P3 in dodecane from method 1, for example, we directly heated P3 at 65 °C for 24 h and then at 75 °C for 16 h. Such a nanoaggregate solution in dodecane was prepared from method 2 by dissolving the diblock in CH_2Cl_2 first. To the CH_2Cl_2 solution was then added dodacane to a volume fraction of 98%. CH_2Cl_2 was removed from the mixture by argon bubbling at 65 °C for 2 h. To ensure similar sample annealing conditions as used in method 1, the dodecane solution freed of CH_2Cl_2 was further heated at 65 °C for 22 h and then at 75 °C for 16 h.

Nanoaggregates vs Micelles. Nanoaggregates prepared as described above in dodecane could be directly aspirated on a carbon-coated copper grid and stained by OsO_4 for TEM observation. TEM images obtained thus contained many deformed spherical particles probably due to the slow evaporation of dodecane during TEM specimen preparation and the low PCEA glass transition temperature T_g of 28 °C.[28] To overcome this difficulty, we photo-cross-linked PCEA, switched dodacane to THF by dialysis, and then added CH to yield a solution of cross-linked nanoaggregates in THF/CH with f_{CH} = 95% before TEM specimen preparation. Figure 1 compares TEM images of cross-linked nanoaggregates prepared initially in dodecane from methods 1 and 2 and aspirated from THF/CH with f_{CH} = 95%. Both methods yielded spherical nanoaggregates with TEM diameters of 81 ± 6 and 28 ± 4 nm, respectively. The fact that the size of the nanoaggregates produced in a given final salvation state depended on the sample history makes the assignment of the thermodynamically favored micelles difficult. For this we have been referring and will refer to all the particles formed in block-selective solvents in this study as nanoaggregates rather than micelles.

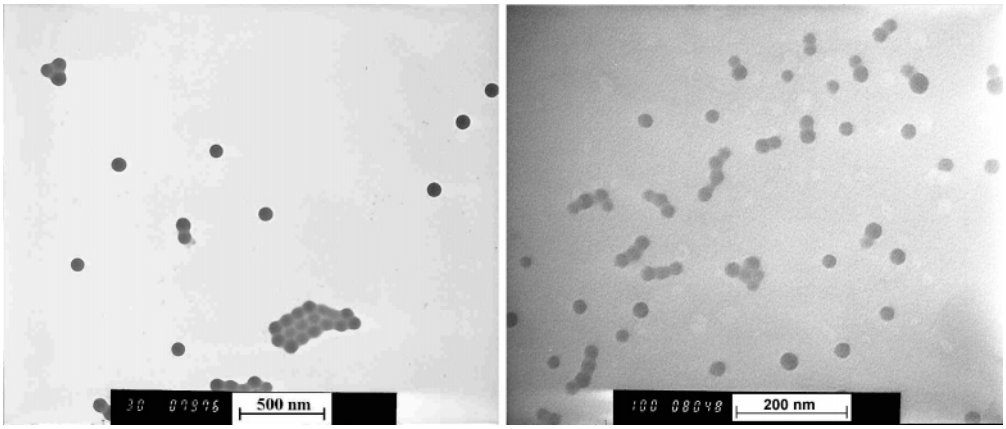

Figure 1. TEM images of P3 nanoaggregates prepared in dodecane from method 1 (left) and 2 (right) and aspirated from THF/CH at $f_{CH} = 95\%$.

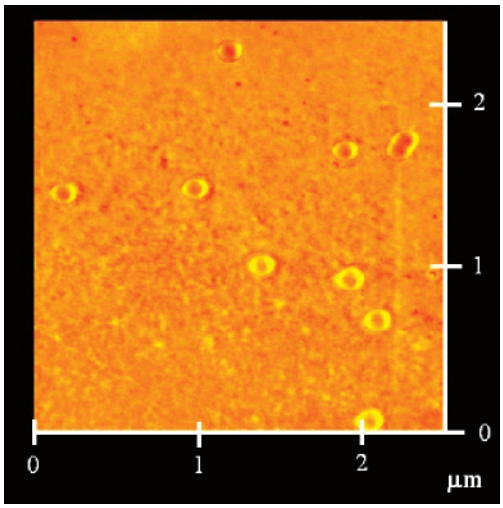

Figure 2. AFM phase image of P3 nanospheres prepared in dodecane from method 1 and aspirated from THF/CH with $f_{CH} = 95\%$.

The fact that we did not end up with spherical nanoaggregates of the same size in dodecane from methods 1 and 2 was surprising because the nanoaggregates were annealed at 75 °C, which was substantially higher than the T_g of 28 °C for PCEA. This could be due to the slow establishment of nanoaggregate size equilibrium for the long PCEA block of P3. Alternatively, PCEA could have cross-linked somewhat during nanoaggregate formation. The possibly different degrees of PCEA cross-linking in the two cases could result in micelles of different sizes.

Core−Shell Nanoaggregates. Nanoaggregates formed in dodecane should possess a PCEA core and a P(EXA−tBA) corona. Surprisingly, such a core−shell structure was not discerned in the TEM images. This might be due to the invisibility of the P(EXA−tBA) chains under our experimental conditions. Figure 2 shows an AFM phase image of P3 nanoaggregates prepared in dodecane by method 1 and aspirated from CH/THF at $f_{CH} = 95\%$. The core−shell structure of such nanoaggregates is evident here with the core diameter at 82 ± 8 nm, in good agreement with the TEM core diameter of 81 ± 6 nm, thus confirming that only PCEA was seen by TEM. The AFM shell diameter was 150 ± 22 nm with a wide distribution because the P(EXA−tBA) shell is very soft and deformed along the horizontal or AFM tip scanning direction.

We have performed also DLS analysis of the P3 nanospheres in THF/CH with $f_{CH} = 95\%$. The hydrodynamic diameter d_h is 138 nm. This is smaller than the AFM shell diameter of 150 ± 22 nm probably because the P(EXA−tBA) shell flattened on mica substrate. Also, the AFM diameter should be larger than that of the flattened particles for the finite size of the AFM tip used.

Table 2. Variation in the DLS d_h of P(EXA−tBA)−PCEA Nanoaggregates Prepared at 22 °C as a Function of f_{CH}

f_{CH} (%)	d_h (nm)	polydispersity K_2^2/K_4
	Nanoaggregates of P1	
80	50	0.041
90	45	0.075
95	46	0.062
98	46	0.076
99.5	79	0.085
100	94	0.093
	Nanoaggregates of P2	
80	46	0.017
99	50	0.095
100	92	0.100

Effect of Binary Solvent Composition Change on Nanoaggregate Size. An objective of this research was to compare lubrication performance of P(EXA−AA)−PCEA nanospheres of different sizes. This subsection discusses how sizes of the P1 and P2 spherical aggregates prepared in THF/CH could be controlled by varying f_{CH}.

As f_{CH} increases, the interfacial tension γ_{CS} between the micellar core and the solvent increases. To decrease the total interfacial energy of the micelles, the size of the micelles should increase and the number of micelles should decrease. This trend has been justified theoretically[40] and verified experimentally.[7,41] We checked the applicability of this strategy to our system despite the fact that our P(EXA−tBA)−PCEA nanoaggregates might not be micelles. Table 2 shows how the DLS diameter d_h and polydispersity K_2^4/K_4 of P1 and P2 aggregates formed in THF/CH changed with f_{CH}.

The d_h values did increase with f_{CH} but the increase did not occur until f_{CH} reached ~99%. Once the d_h started to increase, the increase was steep and pronounced. For P2 nanoaggregates, for example, d_h increased by 42 nm or >80% when f_{CH} changed from 99% to 100%. These are in agreement with the trends shown by polystyrene-*block*-poly(2-cinnamoyloxyethyl methacrylate) nanoaggregates that we studied in THF/CH before[41] and show that the size of P(EXA−tBA)−PCEA nanoaggregates can be tuned over a large range by changing the composition of a binary block-selective solvent mixture.

Size Variation vs Sample Annealing. Table 3 shows how the d_h and K_2^2/K_4 values of P2 nanoaggregates prepared in CH at 22 °C changed after their overnight annealing at higher temperatures. Higher temperature annealing helped reduce both the size and polydispersity of the aggregates somewhat. The size decreased probably for an increased compatibility or a

Table 3. Effect of P2 Nanoaggregate Annealing at Higher Temperatures on Their Size Properties

T (°C)	d_h (nm)	polydispersity K_2^2/K_4
22	92	0.100
55	88	0.081
81	85	0.084

Table 4. Comparison of d_h and K_2^2/K_4 Values of P1−P4 Nanoaggregates Prepared in CH after Heating at 65 °C Overnight

sample	d_h (nm)	K_2^2/K_4
P1	94	0.093
P2	92	0.100
P3	129	0.076
P4	102	0.097

decreased interfacial tension between the PCEA core and heated CH. Aggregate size distribution normally narrows down somewhat at higher temperatures probably for the increased probability for achieving the equilibrium size distributions.

Size Variation with Diblock Copolymer Composition. In singular block-selective solvents, various theoretical[40,42−45] and experimental[18−21] scaling relations exist between the micellar size and the number of repeat units n and m for the soluble and insoluble blocks of a diblock copolymer. Regardless of the scaling relations, the general conclusion is that the aggregation number f should increase with increasing m.

Table 4 compares the DLS size properties of P1−P4 nanoaggregates formed in CH at 65 °C. The fact that P3 possesses the largest m and has also the largest d_h is in agreement with theoretical predictions. Within experimental error samples P1 and P2 have comparable n and m values, and the fact hat they have similar d_h values is also in agreement with theoretical predictions. The d_h value of P4 nanoaggregates is larger than those of P1 and P2 despite the comparable m values of the three samples because n of P4 is substantially larger. Recent numerical analysis of Zhulina et al.[40] indicated that d_h should increase with n at a given m value.

Nanoaggregate Size Variation and Morphology Transition in Singular Block-Selective Solvents. The core size of spherical micelles of a given diblock copolymer should increase as the quality of the block-selective solvent deteriorates for the core block.[40] We have discussed already how to change the quality of binary block-selective solvent mixtures by changing their composition. One can also change the quality of a singular block-selective solvent by switching from one solvent to another. Table 5 summarizes observations that we made of P3 nanoaggregates prepared in different singular solvents. To facilitate a meaningful comparison of sizes of nanoaggregates prepared in different solvents, we irradiated nanoaggregates to achieve a similar CEA double-bond conversion of ∼35% and changed the solvent to THF by dialysis. To such samples were then added CH to achieve $f_{CH} = 95\%$ before DLS and TEM analyses.

The solubility parameter δ of PCEA was calculated to be 20.2 $MPa^{1/2}$. Listed in Table 5 are the solvent δ values that were reported in the literature[46] and calculated by the group contribution method.[39] The δ value of EHC-45 was not calculated for lack of knowledge on its composition. The larger is the difference between δ of PCEA and a solvent, the larger the interfacial tension between the two and thus the larger the core diameter of the aggregates should be.

Both the calculated and the experimental δ values suggest that cyclohexane should be more compatible with PCEA than dodecane, dioctyl ether, and hexane. Interestingly the smallest d_h and d_{TEM} values were determined for the nanoaggregates formed in CH. The d_h and d_{TEM} values were each essentially constant within experimental error for aggregates prepared in dodecane and dioctyl ether. This was again in agreement with the identical δ values calculated for the two solvents. The d_h and d_{TEM} values of aggregates in hexane were not larger than those of aggregates formed in dodecane and dioctyl ether probably for the following reasons. First, the δ values calculated could be erroneous. Second, the nanoaggregates were not necessarily micelles, and the thermodynamic theories of micelles might not hold rigorously for every sample.

Figure 3 shows two TEM images of nanoaggregates formed in EHC-45 oil. P3 evidently formed straight, branched, and looped cylinders in EHC-45 oil. The TEM diameter of the PCEA core of the sample aspirated from THF/CH at $f_{CH} = 95\%$ is 60 ± 7 nm, which is comparable to 62 ± 5 nm found for spherical nanoaggregates formed in CH. Also, one can discern a fuzzy layer around the PCEA core in the right image of Figure 3, confirming the core−shell structure of P(EXA−tBA) and PCEA. The fact that the P(EXA−tBA) layer is so fuzzy confirms also our prior assertion that this layer was not easily discerned by TEM.

According to micellar theories,[40] the gradual deterioration of solvent quality for the insoluble block leads first to spherical micelle size increase and then to morphological transition. After a morphological transition, the core diameter of the particles normally decreases to relieve core chain stretching energy. Such solvent-deterioration-induced morphological tradition has been seen by many groups before.[7,8,47] If micellar theories do apply at all to the P3 aggregates, the fact that we have seen both a morphological transition in the P3 nanoaggregates formed in EHC-45 oil and a decrease in d_{TEM} suggests EHC-45 oil is the least compatible with PCEA of all the solvents examined.

P(EXA−tBA)−PCEA Nanospheres. Cross-linking the PCEA core of the spherical P(EXA−tBA)−PCEA nanoaggregates yielded cross-linked spherical particles, which we have traditionally referred to as nanospheres.[48] PCEA cross-linking was readily achieved via photolysis of the samples by UV light, where PCEA absorbs between ∼260 and ∼340 nm. We monitored the degree of PCEA double-bond conversion by PCEA absorbance decrease at its absorption maximum 274 nm and used a typical double-bond conversion of ∼35% to yield nanospheres. Table 6 summarizes properties of two nanosphere samples that were used for further studies to be discussed below.

Controlled tBA Hydrolysis. We wanted to hydrolyze a fraction β of the tBA groups in the P(EXA−tBA) corona of P(EXA−tBA)−PCEA nanospheres to yield a P(EXA−tBA−AA) corona to examine the effect of β variation on particle lubrication performance. The carboxyl groups were required because they bind strongly with metals and metal oxides as manifested by the use of carboxyl-containing surfactants such as oleic acid to stabilize Co,[49−51] Fe,[52] and γ-Fe_2O_3 nanoparticles.[53] We needed to control β also because too many AA units in the corona of P(EXA−AA)−PCEA nanospheres would lead to their reduced dispersion in lubricant oil.

We established using P5 nanospheres of Table 6 on how to control β by changing tBA hydrolysis time t in CH_2Cl_2/TFA at v/v = 95/5. P5 nanospheres were used in this study because the tBA molar fraction x of this sample was high at 6%, and its ^{1}H NMR peak at 1.46 ppm was sufficiently strong for precise monitoring. We did not use a P(EXA−tBA)−PCEA nanosphere sample with an even higher tBA content because most P(EXA−tBA)−PCEA nanosphere samples used for lubrication tests had x less than 1.5%. At even larger x values, the hydrolysis kinetics may not apply to that of our nanospheres because of the well-known neighbor effect on polymer reactions.

Table 5. Comparison of Size and Morphology of P3 Nanoaggregates Prepared in Different Singular Block-Selective Solvents[a]

solvent	lit. δ (MPa$^{1/2}$)	calcd δ (MPa$^{1/2}$)	morphology of P4 aggregates	DLS d_h (nm)	K_2^2/K_4	d_{TEM} (nm)
cyclohexane	16.8	17.6	spheres	122	0.029	62 ± 5
dodecane	16.2	16.8	spheres	138	0.036	81 ± 6
dioctyl ether		16.8	spheres	135	0.053	75 ± 6
hexane	14.9	16.1	spheres	138	0.045	73 ± 7
EHC-45			branched cylinders			60 ± 7

[a] All the nanoaggregates except those in hexane were prepared by heating P3 in singular solvents at 65 °C for 24 h and then at 75 °C for 16 h. Aggregates in hexane were prepared by heating P3 at 65 °C for 48 h.

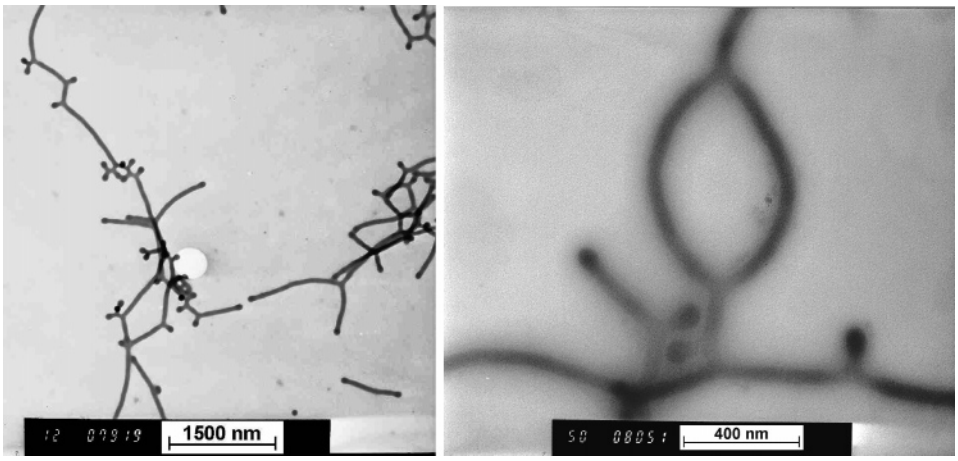

Figure 3. TEM images of P3 nanoaggregates formed and cross-linked in EHC-45. Sample shown on the left was aspirated directly from EHC-45, and sample on the right was aspirated from THF/CH with $f_{CH} = 95\%$. The samples were stained by OsO_4 before TEM observation.

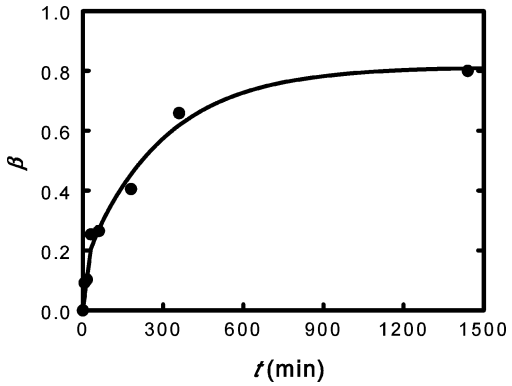

Figure 4. Variation in the degree of tBA hydrolysis β as a function of hydrolysis time t for P5 nanospheres in CH_2Cl_2/TFA with v/v = 95/5.

Table 6. Preparation Conditions and Characteristics of Two Nanosphere Samples That Were Cross-Linked and Used for tBA Hydrolysis, Dispersion, and Adsorption Studies

polymer	prep solvent	prep T (°C)	DLS solvent	d_h (nm)	K_2^2/K_4
P3	CH	60	CH	122	0.016
P5	THF/CH at f_{CH} = 80%	50	CH	83	0.115

Figure 4 shows how β determined from tBA ^{1}H peak decrease changed with the hydrolysis time t for the P5 nanospheres. Fitting the experimental data of Figure 4 yielded the following equation with t in minutes:

$$\beta = 0.8135 - 0.1491e^{-(t/11.7)} - 0.6621e^{-(t/295)} \quad (1)$$

The value β increased with t and approached asymptotically 81% rather 100% at longer times. This incomplete tBA hydrolysis might be real or caused by the relatively large errors involved in tBA peak intensity analysis at higher β values when the residual tBA proton peak was weak. Since we typically use eq 1 to obtain β values less than 60%, the exact cause for $\beta \rightarrow 81\%$ at $t \rightarrow \infty$ under this set of hydrolysis conditions was of little concern to us and was thus not pursued.

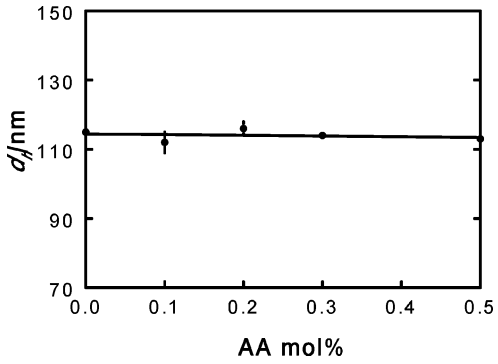

Figure 5. Plot of variation in the hydrodynamic diameter d_h of P1 nanospheres in dodecane as a function of AA mol %.

Effect of Varying AA Contents on Nanosphere Dispersion. Using hydrolysis times calculated from eq 1, we hydrolyzed P3 nanospheres of Table 5 to yield $\beta = 0\%$, 20%, 40%, and 60%. We also obtained a sample with $\beta = 100\%$ by hydrolyzing the nanospheres in CH_2Cl_2/TFA with 25 vol % of TFA for 3 h.[54,55] The nanospheres were then dispersed in THF/dodecane, THF was removed by rota-evaporation, and the DLS d_h values were measured in dodecane as a function of β or AA molar content βx with $x = 0.5\%$. Figure 5 shows results from such an experiment.

The DLS d_h values remained essentially constant or independent of the AA contents up to the highest examined AA content of 0.5 mol %. Since our reasoning is that decreased dispersion of the particles would be marked first by particle clustering and thus a d_h increase, the above results suggest that the spheres at up to 0.5 mol % of AA dispersed well in dodecane.

Ideally, we should have done the above experiment in EHC-45 oil. This was, however, difficult because the high viscosity

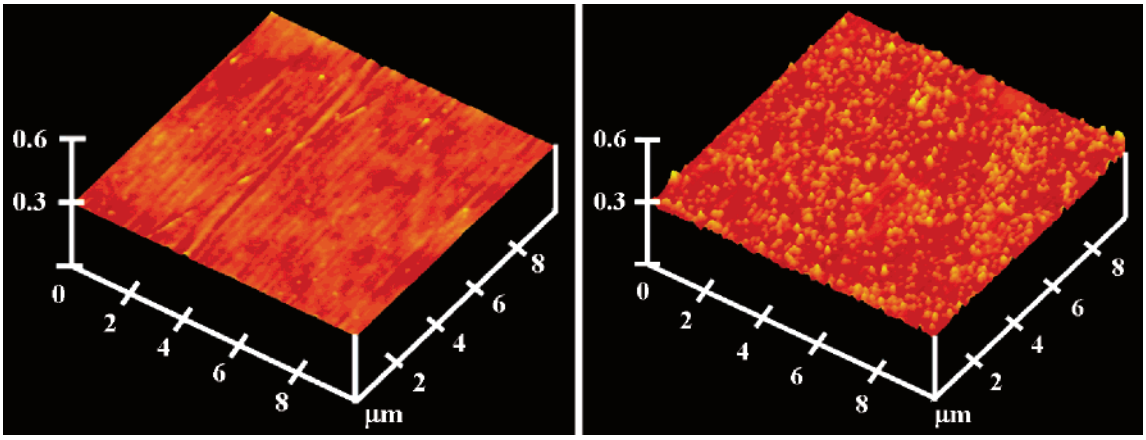

Figure 6. Topography AFM images of stainless-steel surfaces after they were equilibrated with P3 P(EXA−tBA)−PCEA nanospheres (left) and P3 P(EXA−tBA−AA)−PCEA nanospheres with $\beta = 60\%$ (right).

of the oil made sample clarification by filtration for DLS problematic. Dodecane was chosen as a substitute for its known literature refractive index and solvent viscosity values[56] at 25 °C, which are required for DLS d_h evaluation. Despite the possible difference between the critical AA contents above which the P(EXA−tBA−AA)−PCEA spheres start to cluster, the qualitative behavior of the nanospheres in dodacane and EHC-45 should be similar.

Adsorption of P(EXA−tBA−AA)−PCEA Nanospheres. We reasoned that the best way to see whether the AA groups helped promote nanosphere adsorption to stainless-steel surfaces was to compare coverages of polished stainless-steel plates by P(EXA−tBA)−PCEA and P(EXA−tBA−AA)−PCEA nanospheres after such plates had been equilibrated with the nanosphere solutions in EHC-45 oil for some time. Such surface coverages could ideally be probed by fluid AFM or AFM performed of the topography of a submerged surface.[57,58] Unfortunately, EHC-45 is a highly viscous oil, and AFM measurements in such a medium yielded only poor images. Thus, we did most of our experiments in dioctyl ether, which has a much lower viscosity but similar solubility properties as EHC-45 toward the nanospheres.

Figure 6 compares AFM images of stainless-steel surfaces under dioctyl ether after they were equilibrated for 3.5 h with P3 P(EXA−tBA)−PCEA nanospheres or P(EXA−tBA−AA)−PCEA nanospheres with $\beta = 60\%$ at 2.0 mg/mL. While we barely see any adsorbed particles in the former case over a scanned area of $10 \times 10\ \mu m^2$, hundreds of adsorbed P(EXA−tBA−AA)−PCEA spheres are seen in the latter case. Aside from 2.0 mg/mL, we also performed similar studies at nanosphere concentrations of 5.0, 0.50, and 0.1 mg/mL, and the equilibrium P(EXA−tBA−AA)−PCEA adsorption density barely changed with nanosphere concentration. This result demonstrates the superb power of the AA groups in promoting nanosphere adsorption and our success in molecular and nanosphere design.

IV. Conclusions

Nanoaggregates were prepared from five P(EXA−tBA)−PCEA samples. The aggregates were prepared in either singular block-selective solvents or in binary mixtures consisting of a good and block-selective solvent. In the latter case, the size of spherical nanoaggregates prepared from P1 and P2 in THF/CH increased little initially with f_{CH} and then steeply with f_{CH} above $f_{CH} = 99\%$. In the former case changing the singular solvent from CH, the least block selective, to dodecane, dioctyl ether, and hexane increased the core diameter of the P3 spherical nanoaggregtes in agreement with prediction of micellar theory. Changing to EHC-45 oil led to formation of straight, branched, and looped cylindrical aggregates from P3. We have further demonstrated that the nanoaggregates could be cross-linked to yield permanent structures including nanospheres. The tBA groups could be hydrolyzed in a controlled manner to yield nanospheres with different AA contents. At low AA contents, e.g., <0.5 mol %, P3 nanospheres disperse well as individual nanospheres in dodecane. The AA groups have been shown by fluid AFM to promote effectively the adsorption of the nanospheres from the block-selective solvent dioctyl ether on to stainless-steel surfaces. These oil-dispersible and metal-binding spheres should be useful as a friction reduction agent in lubricating oils.

Acknowledgment. Afton Chemical Corp. and the Collaborative Research and Development Program of the Natural Sciences and Engineering Research Council of Canada are gratefully acknowledged for sponsoring this research. G.L. thanks the Canada Research Chairs Program for a chair position in materials science.

References and Notes

(1) Tuzar, Z.; Kratochvil, P. *Surf. Colloid Sci.* **1993**, *15*, 1−83.
(2) Lazzari, M.; Liu, G. J.; Lecommandoux, S. *Block Copolymers in Nanoscience;* Wiley-VCH: Weinheim, Germany, 2006.
(3) Hamley, I. W. *Block Copolymers in Solution: Fundamentals and Applications*; Wiley: Chichester, West Sussex, 2005.
(4) Fustin, C. A.; Abetz, V.; Gohy, J. F. *Eur. Phys. J. E* **2005**, *16*, 291−302.
(5) Hadjichristidis, N.; Iatrou, H.; Pitsikalis, M.; Pispas, S.; Avgeropoulos, A. *Prog. Polym. Sci.* **2005**, *30*, 725−782.
(6) Zhang, L. F.; Eisenberg, A. *Science* **1995**, *268*, 1728−1731.
(7) Cameron, N. S.; Corbierre, M. K.; Eisenberg, A. *Can. J. Chem.* **1999**, *77*, 1311−1326.
(8) Ding, J. F.; Liu, G. J.; Yang, M. L. *Polymer* **1997**, *38*, 5497−5501.
(9) Jain, S.; Bates, F. S. *Science* **2003**, *300*, 460−464.
(10) Li, Z. B.; Kesselman, E.; Talmon, Y.; Hillmyer, M. A.; Lodge, T. P. *Science* **2004**, *306*, 98−101.
(11) Pochan, D. J.; Chen, Z. Y.; Cui, H. G.; Hales, K.; Qi, K.; Wooley, K. L. *Science* **2004**, *306*, 94−97.
(12) Discher, D. E.; Eisenberg, A. *Science* **2002**, *297*, 967−973.
(13) Zhu, J. T.; Liao, Y. G.; Jiang, W. *Langmuir* **2004**, *20*, 3809−3812.
(14) Templin, M.; Franck, A.; DuChesne, A.; Leist, H.; Zhang, Y. M.; Ulrich, R.; Schadler, V.; Wiesner, U. *Science* **1997**, *278*, 1795−1798.
(15) Zhang, L. F.; Yu, K.; Eisenberg, A. *Science* **1996**, *272*, 1777−1779.
(16) Ding, J. F.; Liu, G. J. *Macromolecules* **1999**, *32*, 8413−8420.
(17) Yan, X. H.; Liu, G. J.; Hu, J. W.; Willson, C. G. *Macromolecules* **2006**, *39*, 1906−1912.
(18) Tao, J.; Stewart, S.; Liu, G. J.; Yang, M. L. *Macromolecules* **1997**, *30*, 2738−2745.
(19) Zhang, L. F.; Barlow, R. J.; Eisenberg, A. *Macromolecules* **1995**, *28*, 6055−6066.

(20) Forster, S.; Zisenis, M.; Wenz, E.; Antonietti, M. *J. Chem. Phys.* **1996**, *104*, 9956−9970.
(21) Forster, S.; Abetz, V.; Muller, A. H. E. Polyelectrolyte block copolymer micelles. In *Polyelectrolytes With Defined Molecular Architecture Ii*; 2004; Vol. 166, pp 173−210.
(22) Price, C. *Pure Appl. Chem.* **1983**, *55*, 1563−1572.
(23) Ding, J. F.; Liu, G. J. *Macromolecules* **1997**, *30*, 655−657.
(24) Price, C.; Hudd, A. L.; Stubbersfield, R. B.; Wright, B. *Polymer* **1980**, *21*, 9−10.
(25) Wills, J. G. *Lubrication Fundamentals;* Mercel Dekker: New York, 1980.
(26) Szeri, A. Z. *Tribology, Friction, Lubrication, and Wear;* Hemisphere Publishing Co.: Washington, DC, 1980.
(27) Pugh, B. *Friction and Wear—A Triboloby Text for Students;* Newnes-Butterworths: London, 1973.
(28) Zheng, R. H.; Liu, G. J.; Jao, T. C. *Polymer* **2007**, submitted for publication.
(29) Bataille, P.; SharifiSanjani, N. *Lubr. Eng.* **1995**, *51*, 996−1005.
(30) Guo, A.; Liu, G. J.; Tao, J. *Macromolecules* **1996**, *29*, 2487−2493.
(31) Liu, G. J.; Ding, J. F.; Guo, A.; Herfort, M.; BazettJones, D. *Macromolecules* **1997**, *30*, 1851−1853.
(32) Henselwood, F.; Liu, G. J. *Macromolecules* **1997**, *30*, 488−493.
(33) Erickson, D.; Lu, F. Z.; Li, D. Q.; White, T.; Gao, J. *Exp. Therm. Fluid Sci.* **2002**, *25*, 623−630.
(34) Mehta, A.; Jaouhari, R.; Benson, T. J.; Douglas, K. T. *Tetrahedron Lett.* **1992**, *33*, 5441−5444.
(35) Dong, B. Y.; Manolache, S.; Somers, E. B.; Wong, A. C. L.; Denes, F. S. *J. Appl. Polym. Sci.* **2005**, *97*, 485−497.
(36) Berne, B. J.; Pecora, R. *Dynamic Light Scattering with Applications to Chemistry, Biology, and Physics;* Dover Publications: Mineola, NY, 1976.
(37) Matyjaszewski, K.; Xia, J. H. *Chem. Rev.* **2001**, *101*, 2921−2990.
(38) Liu, G.; Yang, H.; Zhou, J.; Law, S. J.; Jiang, Q.; Yang, G. *Biomacromolecules* **2005**, *6*, 1280−8.
(39) van Krevelen, D. W. *Properties of Polymers—Their Correlation with Chemical Structure; Their Numerical Estimation and Prediction from Additive Group Contributions*, 3rd ed.; Elsevier Science: Amsterdam, 1997.
(40) Zhulina, E. B.; Adam, M.; LaRue, I.; Sheiko, S. S.; Rubinstein, M. *Macromolecules* **2005**, *38*, 5330−5351.
(41) Underhill, R. S.; Ding, J. F.; Birss, V. I.; Liu, G. J. *Macromolecules* **1997**, *30*, 8298−8303.
(42) de Gennes, P. G. Academic Press: New York, 1978.
(43) Halperin, A. *Macromolecules* **1987**, *20*, 2943−2946.
(44) Noolandi, J.; Hong, K. M. *Macromolecules* **1983**, *16*, 1443−1448.
(45) Nagarajan, R.; Ganesh, K. *J. Chem. Phys.* **1989**, *90*, 5843−5856.
(46) Brandrup, J.; Immergut, E. H. *Polymer Handbook*, 3rd ed.; John Wiley & Sons: New York, 1989.
(47) Bang, J.; Jain, S. M.; Li, Z. B.; Lodge, T. P.; Pedersen, J. S.; Kesselman, E.; Talmon, Y. *Macromolecules* **2006**, *39*, 1199−1208.
(48) Ding, J. F.; Tao, J.; Guo, A.; Stewart, S.; Hu, N. X.; Birss, V. I.; Liu, G. J. *Macromolecules* **1996**, *29*, 5398−5405.
(49) Puntes, V. F.; Krishnan, K. M.; Alivisatos, A. P. *Science* **2001**, *291*, 2115−2117.
(50) Black, C. T.; Murray, C. B.; Sandstrom, R. L.; Sun, S. H. *Science* **2000**, *290*, 1131.
(51) Liu, G. J.; Yan, X. H.; Lu, Z. H.; Curda, S. A.; Lal, J. *Chem. Mater.* **2005**, *17*, 4985−4991.
(52) Burker, N. A. D.; Stover, H. D. H.; Dawson, F. P. *Chem. Mater.* **2002**, *14*, 4752.
(53) Hyeon, T.; Lee, S. S.; Park, J.; Chung, Y.; Bin Na, H. *J. Am. Chem. Soc.* **2001**, *123*, 12798−12801.
(54) Yan, X. H.; Liu, G. J.; Haeussler, M.; Tang, B. Z. *Chem. Mater.* **2005**, *17*, 6053−6059.
(55) Lu, Z. H.; Liu, G. J.; Liu, F. T. *Macromolecules* **2001**, *34*, 8814−8817.
(56) Weast, R. C.; Lide, D. R.; Astle, M. J.; Beyer, W. H. *CRC Handbook of Chemistry and Physics*, 70th ed.; CRC Press: Boca Raton, FL, 1989.
(57) Putman, C. A. J.; Vanderwerf, K. O.; Degrooth, B. G.; Vanhulst, N. F.; Greve, J. *Appl. Phys. Lett.* **1994**, *64*, 2454−2456.
(58) Farhan, T.; Azzaroni, O.; Huck, W. T. S. *Soft Matter* **2005**, *1*, 66−68.

MA070901T